INVESTIGATION OF OIL-WATER FLOW IN HORIZONTAL PIPES USING SIMULTANEOUS TWO-LINE PLANAR LASER-INDUCED FLUORESCENCE AND PARTICLE VELOCIMETRY

Ibarra R., Morgan, R., Zadrazil I., Matar O.K. and Markides C.N.*
*Author for correspondence
Department of Chemical Engineering,
Imperial College London,
London SW7 2AZ,
United Kingdom,
E-mail: c.markides@imperial.ac.uk

ABSTRACT

The flow of oil and water in pipes represents a challenging configuration in multiphase flows due to complex hydrodynamics which are still not fully understood. This can be observed in the large number of flow regimes encountered, which extend from smooth stratified flows to complex dispersions such as droplets of oil-in-water and water-in-oil. These flow configurations are the result of the inherent properties of the liquid phases, e.g., their densities and viscosities, interfacial tension and contact angle, as well as of flow conditions and related phenomena, such as turbulence, which have a direct effect on the interface instabilities giving rise to flow regime transitions. In this paper, experimental data are reported that were acquired at low water cuts and low mixture velocities using an aliphatic oil (Exxsol D140) and water as the test fluids in an 8.5 m long and 32 mm internal diameter horizontal pipe. A copper-vapour laser, emitting two narrow-band laser beams, and two high-speed cameras were used to obtain quantitative simultaneous information of the flow (specifically, spatiotemporally resolved fluid-phase and velocity information in both phases) based on simultaneous two-line Planar Laser-Induced Fluorescence (PLIF) and Particle Image and Tracking Velocimetry (PIV/PTV). To the best knowledge of the authors this is the first such instance of the application of this combined technique to these flows. It is found that the rms of the fluctuating velocity show peaks in high shear regions, i.e. at the pipe wall and interface.

INTRODUCTION

Co-current liquid-liquid flow in horizontal pipes is encountered in a range of industrial settings, perhaps most prominently in the oil industry where subsea pipelines transport hydrocarbons and water over hundreds of kilometres. The successful design and operation of such facilities requires reliable predictive simulation software, which is a challenging endeavour as it necessitates a detailed understanding of multiphase flow behaviour.

Liquid-liquid flow has been studied by a number of researchers (see, e.g., Russell *et al.* [1]; Charles *et al.* [2]; Arirachakaran *et al.* [3]; Trallero [4]; Angeli and Hewitt [5], and references therein) in which a wide range of flow regimes have been observed. These flow regimes are strongly dependent on the flow conditions, the fluid properties, and the pipe characteristics (diameter, wettability, and inclination). Flow regimes can be classified into two main categories: separated (e.g., stratified flow), and mixed (e.g., dual continuous). These two main categories can be sub-divided into more detailed configurations, which in some cases can complicate the flow regime classification due to the degree of complexity.

The study of liquid-liquid flows can be performed using a number of measurement techniques, such as quick-closing valves [1,2], pressure transducers [3,4], conductivity or impedance probes [5], high-speed imaging, and wire-mesh sensors. Some of these techniques are intrusive thereby directly affecting the behaviour of the flow and, in turn, increasing the measurement uncertainty, while others can only supply global (or integral) information on the flow and lack the capability of supplying detailed and/or space- and time-resolved information of the *in situ* flow behaviour.

Laser diagnostic techniques offer detailed spatiotemporally resolved *in situ* flow information which is essential for the extraction of important flow quantities such as velocity, Reynolds stresses and turbulence intensities. In particular, Planar Laser-Induced Fluorescence (PLIF) can provide detailed information on the distribution of the two liquid phases in the plane of the laser light, while Particle Image/ Tracking Velocimetry (PIV/PTV) can provide instantaneous local velocity fields in the same plane; these are essential for obtaining velocity profiles, but also to quantify turbulence as well as the near-wall/near-interface velocity shear.

NOMENCLATURE

A	[m^2]	Cross-sectional pipe area
C_w	[m/s]	Interfacial wave velocity
d_h	[m]	Hydraulic diameter
D	[m]	Inside pipe diameter
H	[m]	Height
L	[m]	Length
Q	[m^3/s]	Volumetric flow rate
rms	[-]	Root-mean-squared
Re	[-]	Reynolds number
u	[m/s]	Streamwise velocity component
U	[m/s]	Velocity
WC	[-]	Water cut

Special characters

μ	[Pa.s]	Fluid viscosity
ρ	[kg/m^3]	Fluid density

Subscripts

m	Mixture
max	Maximum
o	Oil phase
T	Total
w	Water phase

PLIF has been employed in previous studies to characterise falling film flows over flat plates [6], co-current downward gas-liquid [7,8] and liquid-liquid annular flows [9], and co-current flows in horizontal pipes [10]. When employing this technique, a plane within the flow is illuminated by a laser light sheet in order to identify the interface between two phases. This is achieved by the addition of a fluorescent dye in one of the phases. The fluorescent dye is excited by the laser light and emits red-shifted light that is then captured by a high-speed camera.

Similarly, PIV and PTV have also been employed in some of the aforementioned studies to obtain instantaneous and averaged velocity-field quantities. Kumara *et al.* [11] employed PIV to characterise the flow structures in oil-water flow in a 56 mm diameter stainless steel pipe, and Zadrazil and Markides [8] made an attempt to provide velocity information in the liquid phase of co-current downward gas-liquid annular flows.

The refractive indices of the fluids (and, less so, pipe solid) play an important role in the implementation of laser-based diagnostic techniques. Distortion of the light sheet occurs when the refractive index between two different liquids is not matched. The refractive indices of the test fluids here (water and Exxsol D60) were not matched. In this case, the laser light is refracted as it passes through the liquid-liquid interface enabling only accurate information in one phase (i.e., before the laser light reaches the interface). Therefore, the experimental procedure was carried out in two steps. Firstly, the flow was illuminated with the laser light sheet from top to bottom to obtain information on the oil phase and, secondly, the laser sheet was introduced from the bottom of the pipe to obtain information in the water phase. This eliminates the possibility of obtaining *simultaneous* information on both phases when the refractive indices of the fluids are not matched and the laser system emits only one laser light. Morgan *et al.* [10] performed experiments in a 25.4 mm internal diameter horizontal stainless steel pipe using Exxsol D80 and a 81.7% wt. glycerol solution. The glycerol solution was selected in order to match the refractive index of the oil phase and avoid refraction of the laser light at the interface. Simultaneous information of both phases was obtained using one laser light sheet. However, the viscosity of the resulting glycerol solution was approximately 43 times higher than the oil phase, which is contrary to what is normally encountered in industrial applications. As a result, the simultaneous PLIF and PIV/PTV for fluids with different refractive indices requires the implementation of a secondary laser light.

This work aims to improve our fundamental understanding of horizontal liquid-liquid flows by the development and application of combined two-line PLIF and PIV/PTV on fluids with similar properties to those encountered in oil transportation systems (refractive indices not matched) using two simultaneous laser light sheets. The data generated can be used to improve the development and validation of advanced computational models for the prediction of multiphase flow in terms of velocity profiles and wall and interfacial shear stresses which can be extracted from the analysis of the velocity gradients and turbulent measurements.

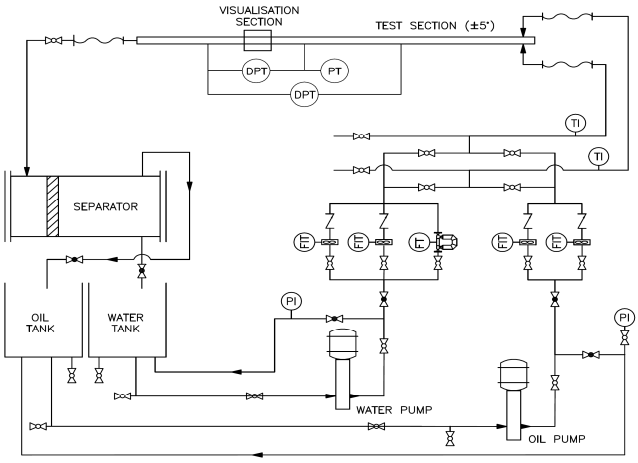

Figure 1 Schematic of the experimental flow facility

EXPERIMENTAL METHODS

Flow facility

The experimental closed-loop flow facility used in this work, shown in Figure 1, is located at Imperial College and allows the study of liquid-liquid flows in horizontal and slightly inclined (±5°) pipes. The flow facility comprises two storage tanks (with a maximum capacity of 680 L each) which are connected to two vertical pumps, each with a nominal capacity of 160 L/min. A set of two turbine flowmeters for each phase (oil and water) are used to measure their volumetric flow rates. The flowmeters have ranges of 2-20 L/min and 14-140 L/min, and an accuracy of ±0.5% of full scale. Additionally, a coriolis mass-flow controller, with a range of 5-300 kg/hr, is installed in the water line to measure low mass flow rates with an accuracy of ±0.2%.

The two liquid phases are introduced into the horizontal test section through a T-junction inlet, as shown in Figure 2. The inlet section consists of a circular channel with an inner horizontal splitter plate, located 10 mm from the bottom of the channel, used to prevent mixing of the two phases before the test pipe. The splitter plate also promotes initially stratified flows. Water and oil are introduced from the bottom and top of the channel, respectively. Additionally, the inlet section is equipped with a flow straightener (perforated plate) and two mesh slots for the purpose of reducing turbulence, secondary flows and making the velocity profile more uniform before the phases flow into the test section.

The test section consists of D = 32 mm *ID* acrylic and fused quartz pipe sections with a total length of 8.5 m. The fused quartz glass pipe is located at the visualisation section and was selected to match the refractive index of the oil phase. Flow measurements were performed at 6.7 m from the inlet such that L/D = 209. The outlet of the test section is connected to a horizontal liquid-liquid separator equipped with a coalescer mesh to enhance separation.

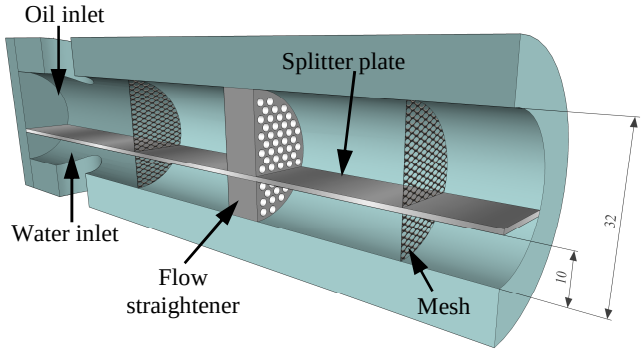

Figure 2 Inlet configuration (dimensions in mm)

Flow conditions and experimental procedure

The liquids used were water (ρ_w = 998 kg/m^3, μ_w = 0.9 mPa.s at 25 °C) and aliphatic oil Exxsol D140 (ρ_o = 825 kg/m^3, μ_o = 5.4 mPa.s at 25 °C) with an interfacial tension of 35.2 mN/m. Experimental data were acquired at low water cuts (WC = 10, 20 and 30%) and low mixture velocities (U_m = 0.3, 0.4 and 0.5 m/s) within the stratified flow regime. The water cut is defined as the volumetric flow rate of water divided by the total volumetric flow rate $WC = Q_w / Q_T$, where $Q_T = Q_o + Q_w$, and the mixture velocities by $U_m = Q_T / A$, with A the pipe cross-sectional area. During each experimental run, the water cut and the mixture velocity were kept constant (steady-state conditions). The temperatures of the fluids during the experiments were measured with K-type thermocouples located upstream of the test section injection point, and were kept

inside the range 22-26 °C. The test section was initially pre-wetted with oil and, then, the water phase was injected to the desired conditions. This was employed to prevent the accumulation of small water droplets at the top of the quartz visualisation section which would distort the laser light. The system was operated and controlled from a LabVIEW® control panel.

Two-line laser system set-up

The set-up of a laser-based diagnostic technique for the study of liquid-liquid flows must take into account the refraction of the laser light as it passes through the test pipe and the liquid phases. Distortion of the laser light can be avoided if the refractive index is matched between the test pipe and both fluids. However, this is a challenging task to accomplish for fluids and pipe materials with properties comparable to those encountered in the field.

The test fluids selected for the experimental investigations have refractive indices of 1.33 (water) and 1.45 (oil/Exxsol D140), respectively. The pipe material was selected to match the refractive index of one of the phases and, therefore, avoid distortion in that phase. It was found that the refractive index of fused quartz glass matched the phase refractive index of the oil phase (Exxsol D140).

The circular shape of the pipe increases optical distortions for the water phase (especially close to the pipe wall) as the refractive indices are not matched. This can be reduced with the use of a rectangular box, made of acrylic and filled with oil, placed around the test pipe and, then, by applying a correction technique based on the imaging of a graticule calibration target.

The difference in the refractive index between both liquid phases requires the implementation of a secondary laser light to obtain simultaneous information on both phases. This is achieved with a copper-vapour laser (Oxford Lasers LS20) which emits two narrow-band laser beams at 510.6 nm (green light) and 578.2 nm (yellow light) with a power ratio of 2:1. The nominal output power of the laser is 20 W at a frequency of 10 kHz. The laser light has a pulse-duration of 2 ns, a pulse energy of 2 mJ, and is delivered to two laser sheet generators using fibre optic cables.

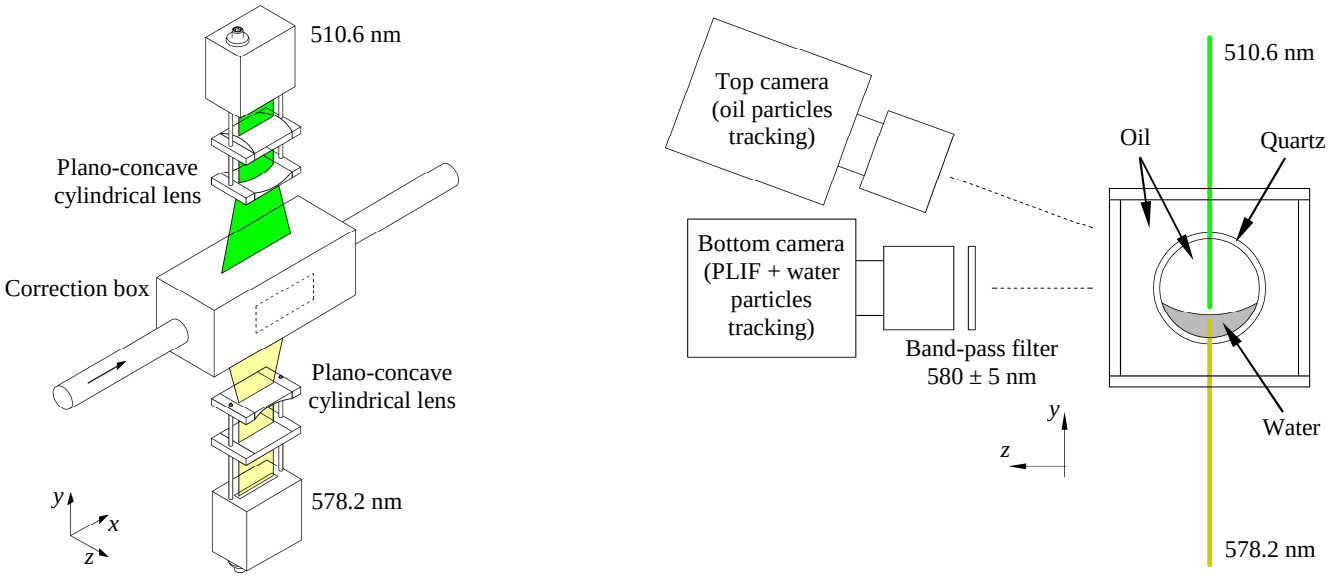

Figure 3 Experimental setup schematics: (a) laser sheet arrangement at the visualisation section, and (b) high-speed camera arrangement

The laser sheet generators were located above (510.6 nm) and below (578.2 nm) the correction box, as in Figure 3a, producing sheets of approximate thickness 1 mm at the test pipe. The width of the illuminated regions were expanded using plano-concave cylindrical lenses, coverage of the entire camera viewing window.

PLIF requires a clear distinction between the liquid phases which is achieved by adding a fluorescent dye. The selection of the fluorescent dye must take into account the excitation and emission spectra with respect to the laser light in order to increase the brightness enabling identification the liquid-liquid interface. It was found that the fluorescent dye Eosin Y can be excited at 510 nm (green laser light) and has no excitation at 578 nm (yellow laser light). A concentration of 0.075 mL of a 5 % wt. solution of Eosin Y per litre of water was used in the experimental campaign.

The *in situ* phase velocities can be determined by tracking seeded particles in the flow in consecutive images. These particles must be small enough to follow the direction of the flow and be able to scatter enough light to be captured by the high-speed cameras. Kumara *et al.* [11] employed polyamide particles with a mean particle diameter of 20 μm and a density of 1.03 g/cm^3. Poulin *et al.* [12] used fluorescent PMMA particles encapsulated with Rhodamine B with a particle diameter range between 1-20 μm and a density of 1.18 g/cm^3 for the study of flow of heptane and 43 % wt. glycerol solution in a horizontal pipe. In this work, hollow glass spheres, with a mean particle diameter of 10 μm and a density of 1.1 g/cm^3, and silver coated glass spheres, with a mean particle diameter of 50 μm and a density of 0.8 g/cm^3, were seeded in the water and oil phase, respectively.

The scattered light from the seeded particles and fluorescent emission from the dye were captured by two high-speed cameras, as shown in Figure 3b. The bottom camera, an Olympus iSpeed 3 with a maximum resolution of 1280×1024 pixels at a maximum frame-rate of 2000 fps, was used to capture the light from the fluorescent dye and the scatter light from the seeded particles in the water phase at 578.2 nm. A band-pass filter at 580 ± 5 nm was used for the bottom camera. The top camera, an Olympus iSpeed 2 with a maximum resolution of 800×600 pixels at a maximum frame-rate of 1000 fps, captured the scatter light from the seeded particles in the oil phase and the fluorescent emission from the dye which was later removed by a masking procedure.

Synchronised images were recorded over 5 s at 500 Hz and 1 kHz for the top and bottom cameras, respectively. The laser frequency was kept at 10 kHz to maximise illumination. This means that no synchronisation between the laser and the imaging system was employed resulting in multi-exposures per image.

Image Processing

The first step in the processing of the images involves the correction for optical distortion due to the circular shape of the pipe and the angle of incidence of the camera. This operation was performed using LaVision's DaVis 8.3 software. A calibration target was introduced into the test pipe, as shown in Figure 4, in which the flat surface of the graticule was aligned with the plane of the laser light sheet. The pipe was filled with water to calibrate the bottom camera images and oil to calibrate the top camera images. The target consists of crosses of a known size and separation distance, used to measure the distortion of the recorded image.

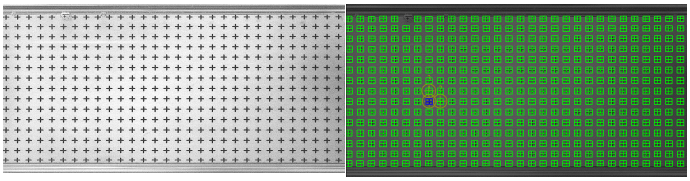

(a) **(b)**

Figure 4 Graticule correction process: (a) target raw image from the bottom camera (pipe filled with water), and (b) distortion correction process (crosses detection)

Once the images have been corrected for distortion, PLIF processing can be applied to the bottom camera images. The scattered light from particles in the oil layer and reflections above the interface are removed using an image processing algorithm in MATLAB. Results of the image processing are shown in Figure 5. Interface profiles and instantaneous and time-averaged phase fraction profiles can then be determined.

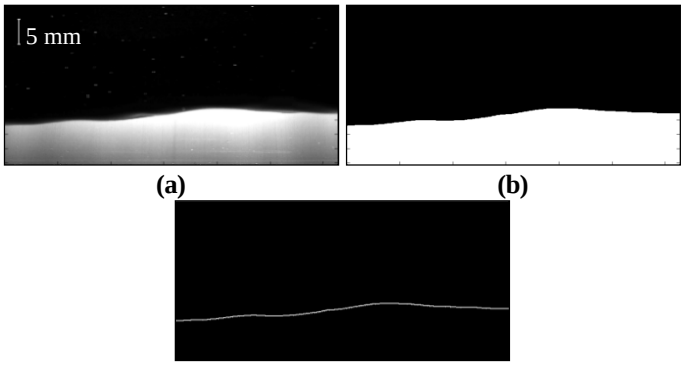

(a) **(b)**

(c)

Figure 5 PLIF image-processing: (a) raw instantaneous image, (b) binarised image, and (c) instantaneous interface profile

The instantaneous interface profile obtained from the PLIF analysis (bottom camera images) is used to mask the corresponding image from the top camera in order to remove any reflections below the interface and fluorescence emission from the water layer (see Figure 6) that could interfere with the particle tracking process. The interface profile from the bottom camera must be scaled in the horizontal and vertical axes to be adapted to the images from the top camera. This is performed by using the graticule target as the scaling reference plane.

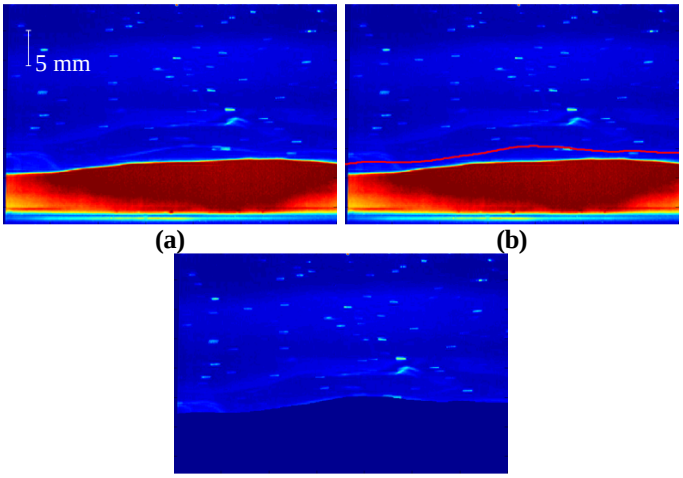

(a) **(b)**

(c)

Figure 6 Top camera image-processing: (a) raw instantaneous image, (b) scaled interface profile (red line) from the bottom camera image for masking of (a), and (c) masked image

The tracking of the seeded particles in the flow, in order to obtain instantaneous velocity vector maps, was performed in two steps. In the first step, PIV was applied to the recorded images to obtain a reference vector field that, in a second step, was used for the PTV processing to determine the final velocity field of the flow. The PIV processing was performed independently for each liquid phase using the DaVis 8.3 software. The initial and final interrogation windows, with 50% overlap, were selected to be 128×128 and 48×48 pixels, respectively. The velocity vectors from the PTV analysis were calculated within an 8×8 pixel interrogation window. The same parameters were used for both phases. Figure **7** demonstrates of the PIV/PTV processing steps performed on the recorded images. Finally, time-averaged quantities are determined from the instantaneous velocity vectors.

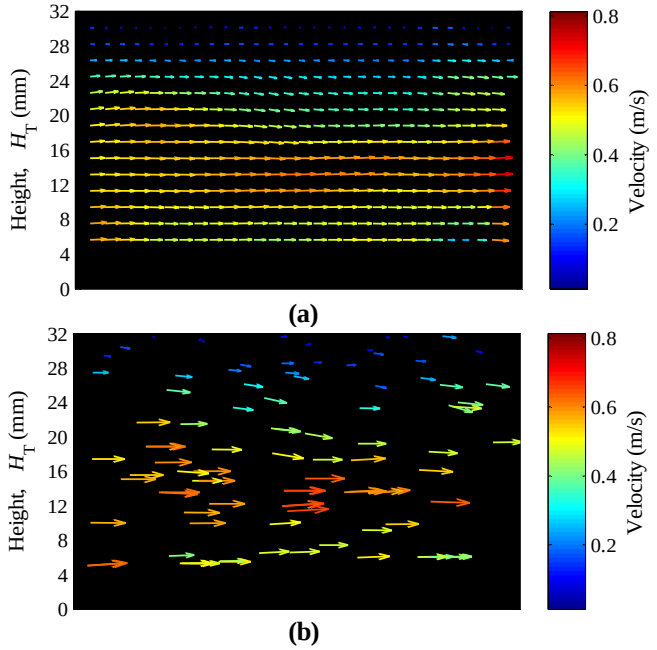

(a)

(b)

Figure 7 Example processed PIV/PTV results: (a) instantaneous PIV, and (b) instantaneous PTV velocity vector maps

RESULTS

The simultaneous two-line laser-based diagnostic technique can only be implemented accurately in stratified flows. When a large number of droplets of one phase are encountered in the bulk of the other phase, the laser sheet is refracted as it passes through the multiple interfaces. The flow was observed to be in the stratified-smooth or stratified-wavy regime for the flow conditions studied here; in this set of experiments, the wave amplitude increases with the mixture velocity.

Velocity profiles

Figure 8 shows mean streamwise velocity component profiles for water cuts (*WC*) of 10% and 30% and different mixture velocities. The velocity profiles are normalised by the respective mixture velocities. For *WC* = 10% (Figure 8a), the velocity profiles appear to collapse at the bottom section of the pipe (H_T < 6 mm). This region corresponds to the water layer in which the Reynolds number ranges from *Re* = 4300 for U_m = 0.3 m/s to *Re* = 6700 for U_m = 0.5 m/s. (The Reynolds number is defined as $Re = \rho U d_h/\mu$ where *U* is the average *in situ* fluid velocity of a particular phase.) This trend, which is also observed for *WC* = 30% for H_T < 10 mm (Figure 8b), indicates that the normalised velocity profiles in the water layer are largely independent of the mixture velocity.

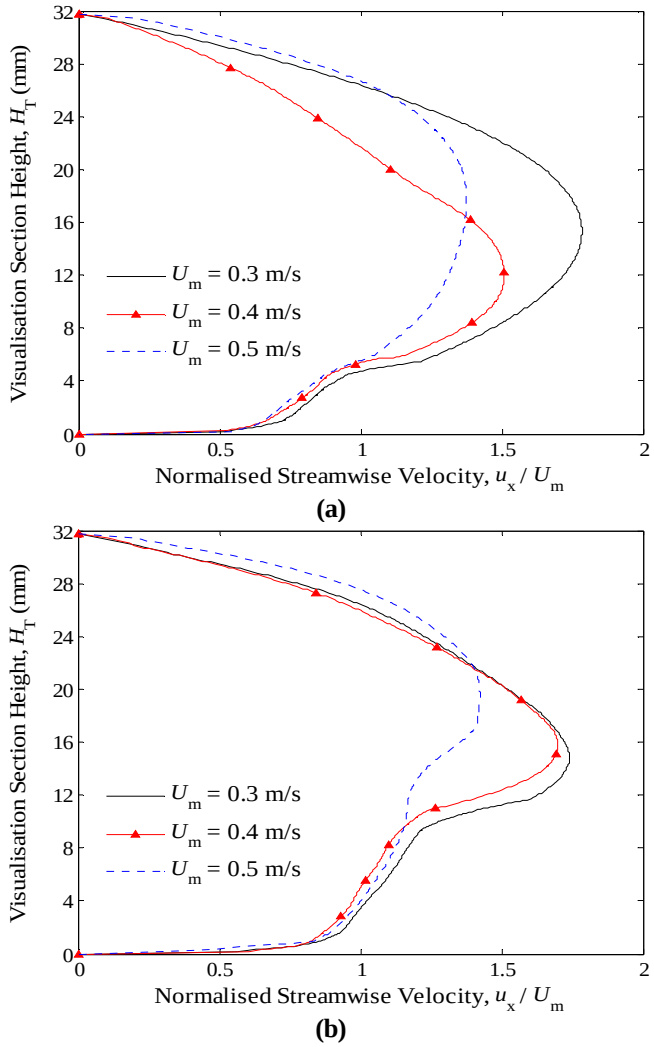

Figure 8 Normalised mean streamwise velocity profiles for: (a) *WC* = 10% and (b) *WC* = 30%

On the other hand, the velocity profiles in the oil phase (at the upper part of the pipe section) vary for different mixture velocities. Parabolic profiles are observed for U_m = 0.3 m/s and 0.4 m/s, where the local *Re* are 1950 and 2400, respectively. However, the maximum mean streamwise velocity is encountered at different heights from the bottom of the pipe. This difference is more noticeable in the lower water-cut (*WC* = 10%) flow, for which $H_T|_{u_{max}}$ = 15.3 mm for U_m = 0.3 m/s and $H_T|_{u_{max}}$ = 12.0 mm for U_m = 0.4 m/s. For U_m = 0.5 m/s, the mean streamwise velocity shows a flatter profile compared to the other flows.

It can be observed that the oil phase flows at a higher velocity than the water layer at the bottom (lower section) of the pipe. However, the velocity at the interface must be similar for both phases in order to keep the continuity criterion. This results in a sharp velocity gradient located at the oil-water interface which may be located in an interfacial boundary layer. The velocity of the flow in this interfacial boundary layer region in either one or both phases changes in a similar approach than the wall boundary layer. The velocity transition at the interface becomes smoother with increasing mixture velocity for which the normalised maximum streamwise velocity in the oil layer decreases and the amplitude of the interfacial waves increases.

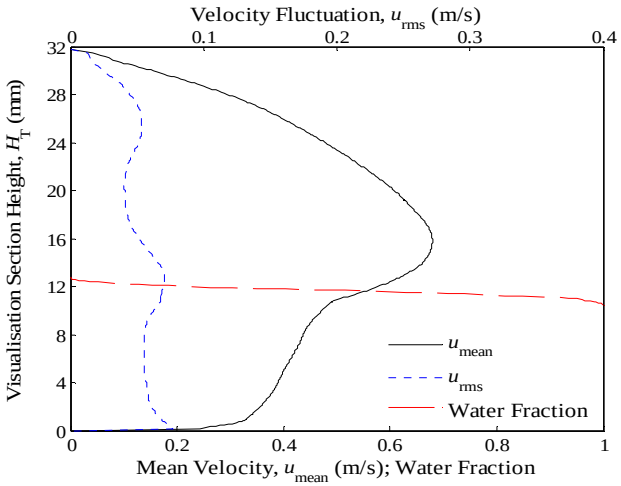

Figure 9 Mean and rms axial velocity (*WC* = 30%, U_m = 0.4 m/s)

Interfacial wave speeds were estimated from cross-correlations of the interfacial height between two different streamwise locations. The velocities of the interfacial waves are also found to differ for the two water-cut flow cases studied. For *WC* = 10%, the average wave-velocities are lower than the corresponding mixture velocity (C_w/U_m = 0.89 to 0.97). This corresponds with the trend of the obtained velocity profiles in which the sharp transition is observed at approximately u_x/U_m = 1. For *WC* = 30%, the normalised average wave-velocity is larger than 1, as observed in the velocity profiles in Figure 8b. This behaviour can be attributed to the interaction of the faster flowing phase over the slower phase which acts as a dragging force over the top layer of the water phase. For *WC* = 30%, the maximum mean streamwise velocity in the oil layer is located closer to the liquid-liquid interface than *WC* = 10%. As a result, higher normalised velocities are observed at the top layer of the water phase for *WC* = 30%. Moreover, interfacial waves increase in amplitude as increasing the water cut due to an interaction of the faster flowing phase.

The turbulence levels in the flow can be characterised by the magnitude of the streamwise velocity fluctuations (u_{rms}). Close to

the pipe wall, u_{rms} exhibits a peak, as it does near the interface, at which locations large mean velocity gradients are found. This behaviour is clearly in Figure 9 for WC = 30% and U_m = 0.4 m/s.

A secondary peak in the velocity fluctuations is observed near the liquid-liquid interface. This could be the result of instabilities at the interface which are generated by the interfacial shear. These instabilities are enhanced with the mixture velocity due to the effect of larger waves at the interface. Moreover, the profile of the velocity fluctuations indicates the locations where the shear is decreased or zero ($\partial u_{mean}/\partial y = 0$). This is represented by the valleys in the u_{rms} profile in oil and water layers.

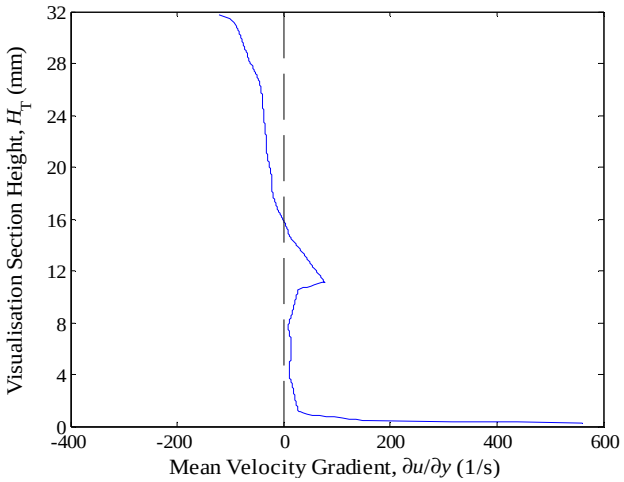

Figure 10 Mean axial velocity gradient (WC = 30%, U_m = 0.4 m/s)

Interfacial shear stresses can be evaluated from the velocity gradients in the near-interface region. This information is of great importance in the characterisation of liquid-liquid flows as it provides an insight of the mechanisms involve in breakup and droplet generation that leads to flow regime transitions (i.e., from stratified to non-stratified flows). The addition of Reynolds stresses information to the evaluation of interfacial shear stresses would provide a more accurate interpretation as it would include the effect of secondary flows at the interface. The extraction of the fluctuating velocity in liquid-liquid flow is, therefore, key to improving our understanding of these flows. An accurate evaluation of the interfacial shear stresses would improve prediction of flow parameters such as the pressure drop. Current models evaluate the interfacial shear stresses based on: empirical correlations, a fraction of the wall shear stress of one of the phases, or a fixed value [13]. These types of approximations do not yield to accurate predictions of the *in situ* phase fractions and pressure drop for a wide range of flow conditions and pipe configurations.

CONCLUSION

Experimental investigations were conducted in a 32 mm *ID* horizontal pipe to study the hydrodynamics of stratified oil-water flows. A combination of simultaneous two-line laser-based diagnostic techniques, namely, Planar Laser-Induced Fluorescence and Particle Image/Tracking Velocimetry, were employed to characterise the *in situ* interface profile, mean axial and fluctuating velocity profiles. For this, a system comprising a Cu-vapour laser with two narrow-band laser light beams and two high-speed cameras was used to capture instantaneous images of the flow.

While it is true that the implementation of two laser light sheets allows the study of fluids with different refractive indices, the technique is limited, generally, to separated flows (i.e., stratified or stratified-wavy flows) as the occurrence of droplets of one phase in the bulk of the other would result in refraction of the light increasing the measurement uncertainty.

The mean velocity profiles show characteristics of laminar and turbulent flow for the conditions studied and interesting interactions between the two co-flowing phases. Normalised velocity profiles indicate that the mean axial velocity for the water phase is independent of the mixture velocity for given water cut. The level of turbulence in the flow was characterised by the rms of the fluctuating velocity components in the axial direction, showing peaks in regions of high shear, i.e., close to the pipe wall and at the liquid-liquid interface. The generated information can be further employed to evaluate interfacial shear stresses which are crucial in facilitating our understanding of the underlying interfacial phenomena and the development of advanced models.

ACKNOWELDGEMENTS

This work has been undertaken within the Consortium on Transient and Complex Multiphase Flows and Flow Assurance (TMF). The authors gratefully acknowledge the contributions made to this project by the UK Engineering and Physical Sciences Research Council (EPSRC) through a Programme Grant (MEMPHIS, EP/ K003976/1) and the following: ASCOMP, BP Exploration; Cameron Technology & Development; CD adapco; Chevron; KBC (FEESA); FMC Technologies; INTECSEA; Granherne; Institutt for Energiteknikk (IFE); Kongsberg Oil & Gas Technologies; MSi Kenny; Petrobras; Schlumberger Information Solutions; Shell; SINTEF; Statoil and TOTAL.

REFERENCES

[1] Russel, T.W.F., G.W. Hodgson, and G.W. Govier, Horizontal pipeline flow of mixtures of oil and water, *Can. J. Chem. Eng.*, Vol. **37** (1), 1959, pp. 9-17

[2] Charles, M.E., G.W. Govier, and G.W. Hodgson, The horizontal pipeline flow of equal density oil-water mixtures, *Can. J. Chem. Eng.*, Vol. **39** (1), 1961, pp. 27-36

[3] Arirachakaran, S., K.D. Oglesby, M.S. Malinowsky, O. Shoham, and J.P. Brill, An analysis of oil/water phenomena in horizontal pipes, *SPE Paper 18836, SPE Prod. Oper. Symp.*, Oklahoma City, March 13-14, 1989, pp. 155-167

[4] Trallero, J.L., Oil-Water Flow Pattern in Horizontal Pipes, *Ph.D. Thesis*, The University of Tulsa, 1995

[5] Angeli, P., and G.F. Hewitt, Flow structure in horizontal oil-water flow, *Int. J. Multiph. Flow*, Vol. **26** (7), 2000, pp. 139-157

[6] Charogiannis, A., J.S. An, and C.N. Markides, A simultaneous planar laser-induced fluorescence, particle image velocimetry and particle tracking velocimetry technique for the investigation of thin liquid-film flows, *Exp. Thermal and Fluid Sci.*, Vol. **68**, 2015, pp. 516-536

[7] Schubring, D., A.C. Ashwood, T.A. Shedd, and H. E.T., Planar laser-induced fluorescence (PLIF) measurements of liquid film thickness in annular flow. Part I: Methods and data, *Int. J. Multiph. Flow*, Vol. **36**, 2010, pp. 10

[8] Zadrazil, I., and C.N. Markides, An experimental characterization of liquid films in downwards co-current gas-liquid annular flow by particle image and tracking velocimetry, *Int. J. Multiph. Flow*, Vol. **67**, 2014, pp. 12

[9] Liu, L., Optical and computational studies of liquid–liquid flows, *Ph.D. Thesis*, Imperial College London, 2005

[10] Morgan, R.G., C.N. Markides, I. Zadrazil, and G.F. Hewitt, Characteristics of horizontal liquid–liquid flows in a circular pipe

using simultaneous high-speed laser-induced fluorescence and particle velocimetry, *Int. J. Multiph. Flow*, Vol. **49**, 2013, pp. 99-118
[11] Kumara, W.A.S., B.M. Halvorsen, and M.C. Melaaen, Particle image velocimetry for characterizing the flow structure of oil-water flow in horizontal and slightly inclined pipes, *Chem. Eng. Sci.*, Vol. **65**, 2010, pp. 4332-4349
[12] Conan, C., O. Masbernat, S. Decarre, and A. Line, Local hydrodynamics in a dispersed-stratified liquid-liquid pipe flow, *AIChE*, Vol. **53** (11), 2007, pp. 15
[13] Taitel, Y., D. Barnea, and J.P. Brill, Stratified three phase flow in pipes, *Int. J. Multiph. Flow*, Vol. **21** (1), 1995, pp. 8